Journal of Structural Geology, Vol. 8, No. 1, pp. 35 to 46, 1986
Printed in Great Britain

0191-8141/86 $03.00 + 0.00

Strain and displacement across the Pinaleño Mountains shear zone, Arizona, U.S.A.

STEPHEN J. NARUK

Department of Geosciences, University of Arizona, Tucson, AZ 85721, U.S.A.

(*Received* 23 *October* 1984; *accepted in revised form* 29 *March* 1985)

Abstract—The 27 km long, 0.5 km thick mylonite zone of the Pinaleño Mountains metamorphic core complex is interpreted as a normal-displacement simple-shear zone on the basis of major, minor and microscopic-scale structures. Shear strains calculated as a function of the angle between the foliation and the lower boundary of the shear zone range from 2 to 19 and have a mean value of 3.5, corresponding to a mean angular shear of 74°. These values are the same as those calculated independently from rotations of sheared lithologic contacts. Integration of the calculated shear strains yields a minimum translation estimate of 2.9 km.

INTRODUCTION

THE PINALEÑO Mountains are a NW-trending range within the Basin and Range Province of southeastern Arizona. The Pinaleño shear zone is a planar zone of mylonitic rocks, approximately 27 km long and 0.5 km thick, which trends northwestward and dips moderately northeastward along the northeast flank of the range (Fig. 1). When projected up-dip to the southwest, the zone projects over the peaks of the range.

The age and original orientation of the zone are controversial. Davis (1980a) and Rehrig & Reynolds (1980) interpret the zone as one of several low-angle, normal-displacement, mylonitic tectonite zones of mid-Tertiary age, and associated with metamorphic core complexes. Davis (1980a), Rehrig & Reynolds (1980), Davis & Hardy (1981) and Spencer (1984) interpret the Pinaleño mylonites as the deep crustal continuation of low-angle normal faults which truncate Oligocene dikes and extrusives. In contrast, C. Thorman (personal communication, 1984) maintains, on the basis of unpublished data, that the zone was a SW-dipping thrust in Mesozoic or early Tertiary time. He believes that the present northeast dip of the zone is due to post-kinematic rotation of the zone by unspecified structures.

Because the Pinaleño Mountains have been interpreted as a metamorphic core complex, the kinematics of the Pinaleño zone are controversial as well. In the sense originally used by Davis & Coney (1979), a metamorphic core complex consists of a crystalline core,

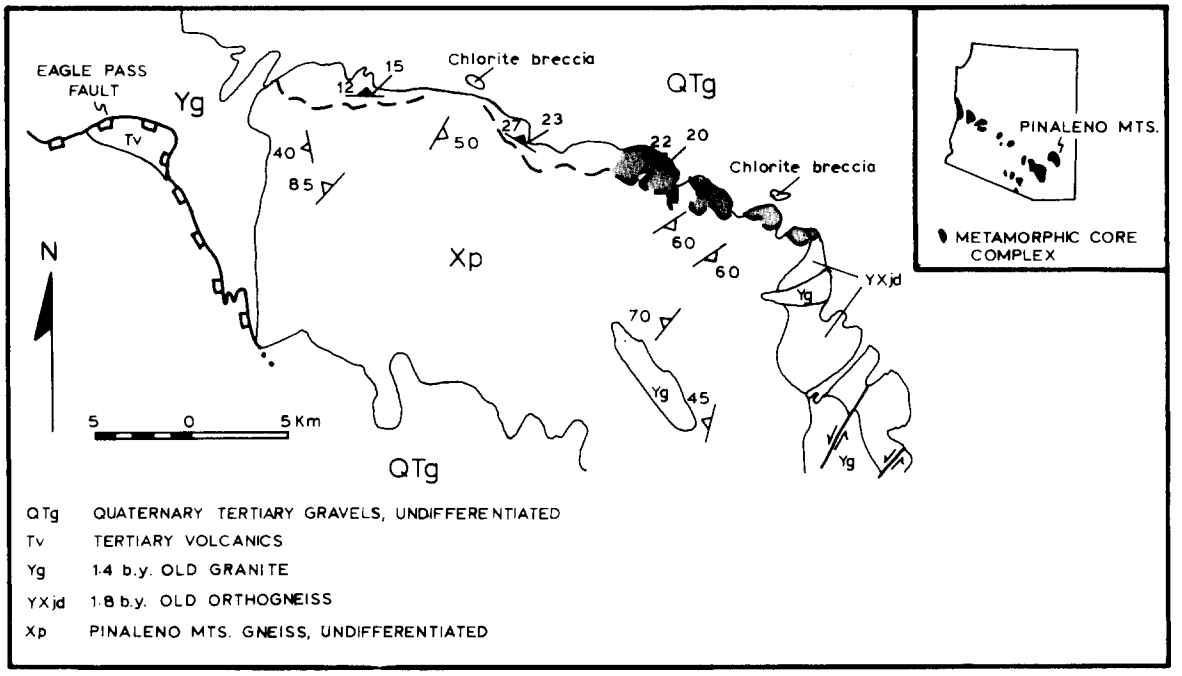

Fig. 1. Generalized geologic map of the Pinaleño Mountains, with inset showing location of Pinaleño Mountains relative to other Arizona metamorphic core complexes. Shaded area represents the part of the zone shown in detail in Fig. 3. Open symbols represent crystalloblastic foliation. Solid symbols represent mylonitic foliation and lineation. Heavy dashed line represents shear zone boundary. (Compiled from Bergquist 1979, Blacet & Miller 1978, Davis 1980a, Davis & Hardy 1981, Thorman 1982, plus original research. Inset after Coney 1980).

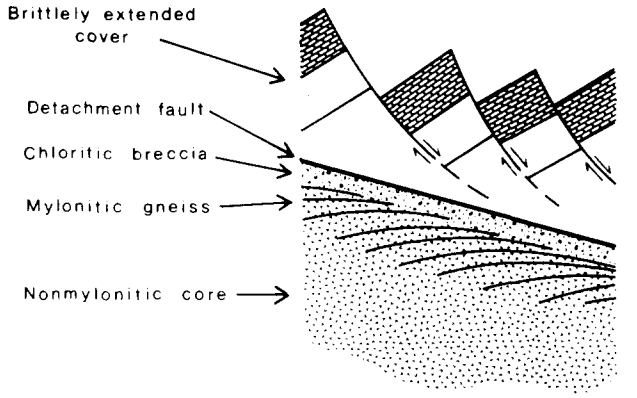

Fig. 2. Schematic vertical cross-section of a metamorphic core complex (after Davis 1980a).

a mylonitic carapace, a décollement, and a brittlely extended cover or suprastructure (Fig. 2). In general, the mylonites within such complexes have been interpreted as products of thrust-slip shear (e.g. Misch 1960, Davis *et al.* 1980, Brown & Read 1983), as products of megaboudinage-like extension and necking of the entire crust (Davis & Coney 1979, Davis 1980a), as products of pure-shear extension of the upper crust exclusively (Miller *et al.* 1983), and as products of normal-slip simple shear (Davis 1980b, 1983).

In general, the orientation of θ' foliation in a domain of shear can be described as some function of simple shear, pure shear, and volume change (Ramsay 1980). The present paper demonstrates that shear strains and an estimate of minimum translation within the Pinaleño mylonite zone can be calculated from the following equations which assume that simple shear is the only variable:

$$\text{shear strain, } \gamma = 2 \operatorname{cotan} 2\theta', \tag{1}$$

$$\text{translation, } S = \int_0^x \gamma \, dx, \tag{2}$$

where θ' equals the angle between the macroscopic foliation and the shear zone boundary (Ramsay & Graham 1970). Shear strain and the principal elongations (e_1, e_2, e_3) in turn are related by the following equations (Ramsay 1980)

$$(1 + e_1)^2 = \tfrac{1}{2}[2 + \gamma^2 + \gamma(\gamma^2 + 4)^{1/2}], \tag{3}$$

$$e_2 = 0, \tag{4}$$

$$(1 + e_3)^2 = \tfrac{1}{2}[2 + \gamma^2 - \gamma(\gamma^2 + 4)^{1/2}]. \tag{5}$$

The conclusion that simple shear analysis can be successfully applied to a metamorphic core complex is diametrically opposed to the conclusion drawn from the only other quantitative strain study of such a complex (Miller *et al.* 1983). It also differs significantly from the conclusions of a number of other shear zone studies, and thus has important implications for shear zone studies in general. The Ramsay & Graham (1970) model has been applied successfully to numerous outcrop-scale shear zones (e.g. Ramsay & Graham 1970, Ramsay & Allison 1979, Mitra 1979, Ramsay 1980). Attempts to apply the model quantitatively to km-scale zones are rare, however, and generally unsuccessful. Escher *et al.* (1975) note that the strain within a regional Precambrian thrust-slip shear zone is not a plane strain, although they assume plane-strain deformation in order to estimate strain values. Kligfield *et al.* (1981) report that the strains measured in a regional Apennine thrust-slip shear zone can only be explained as the combined product of simple shear, pure shear, and volume change.

Others have indicated that the Ramsay & Graham (1970) model may not be quantitatively applicable on any scale. Coward (1976) argues that the inevitable termination of a shear zone requires that the deformation within the zone involve both pure shear and simple shear components. Berthé *et al.* (1979) and Lister & Snoke (1984) suggest that the presence of spaced, microscopic zones of apparently high displacement within some mylonites ('C' or *cisaillement* surfaces) indicates that the macroscopic foliation within the shear zone does not represent the plane of finite strain for the bulk rock. Lister & Snoke (1984) particularly suggest that, in SC-mylonites of the type described below, the dominant foliation is related to shear surfaces and not to the finite strain plane.

GEOLOGY OF THE PINALEÑO MOUNTAINS MYLONITE ZONE

Description of the mylonites' protoliths

The rocks structurally below the mylonite zone consist of quartzofeldspathic gneiss, biotite schist, coarsely porphyritic orthogneiss, granodiorite and granite (Fig. 3). Layers of amphibolite, quartzite and pelitic schist occur locally within the quartzofeldspathic gneiss and biotite schist, but do not represent map-scale units. The granite and granodiorite are undeformed outside the mylonite zone. The metamorphic rocks contain a crystalloblastic foliation that strikes NE and dips moderately to shallowly SE within a few kilometers of the mylonite zone (Fig. 4a). Elsewhere in the range the strike is commonly NE, but locally variable, and the dip is subvertical (Swan 1976, C. Thorman, personal communication 1984). No crystalloblastic lineation is present. Contacts between the metamorphic rock types are sharp rather than gradational, and are parallel to the local crystalloblastic foliation.

Description of the mylonites

All of the above rock types can be traced continuously from southwest to northeast into the mylonite zone, where they develop a pervasive mylonitic foliation and lineation. Contacts, which trend NE in the unsheared rocks, remain NE-trending in the mylonitic rocks, parallel to the principal extension direction defined by the mylonitic lineation.

The mylonitic foliation strikes 315–285° and typically dips 10–25° NE throughout the shear zone (Fig. 4b); the lineation uniformly trends 040° (Fig. 4c). Locally, the foliation at the base of the zone may be horizontal or SW-dipping. In the higher structural levels the foliation

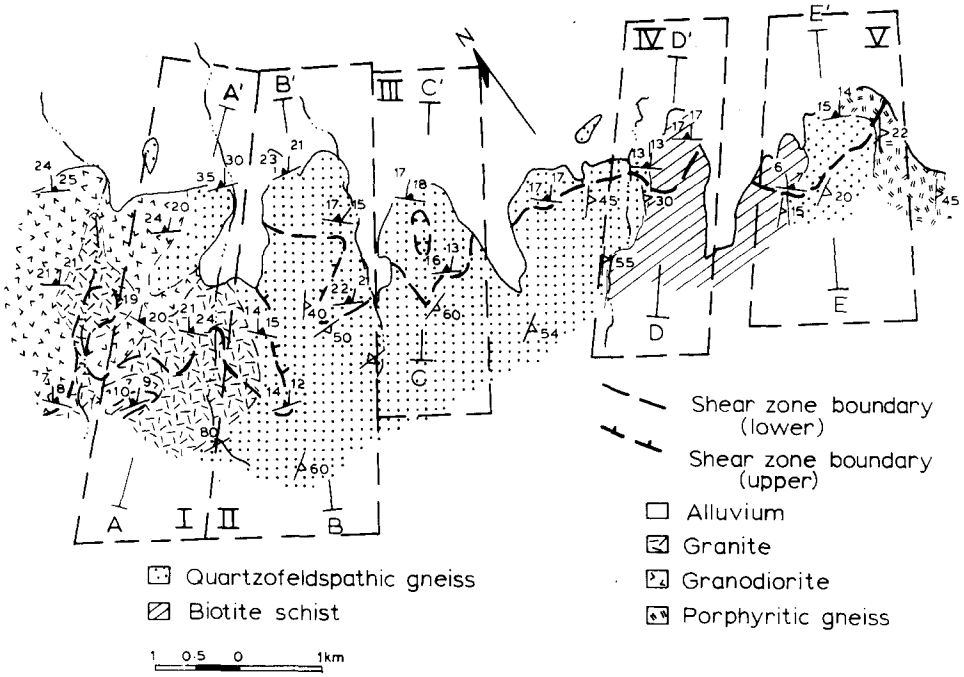

Fig. 3. Detailed geologic map of a part of the Pinaleño Mountains shear zone. Symbols as in Fig. 1. Approximate boundaries of structural domains I–V are indicated by screened dashed lines.

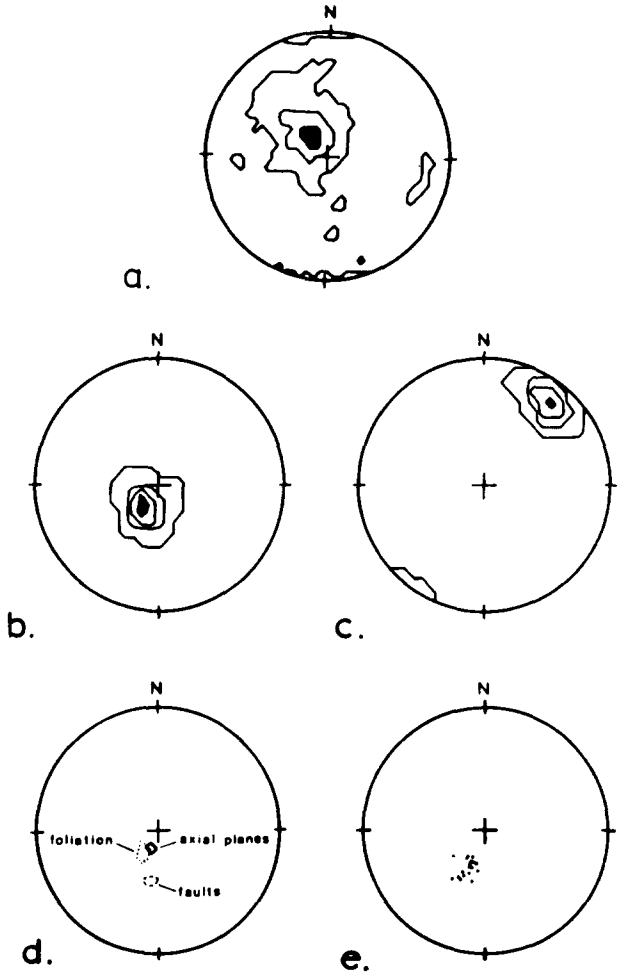

Fig. 4. Lower hemisphere, equal-area projections of (a) poles to crystalloblastic foliation (contours equal 1, 5, 10% of data points per 1% area); (b) poles to mylonitic foliation (contours equal 1, 10, 20, 40% of data points per 1% area); (c) mylonitic lineations (contours equal 1, 10, 20, 40% of data points per 1% area); (d) 40% contours of poles to mylonitic foliation, poles to fault planes, and poles to fold axial planes; (e) poles to shear-zone lower boundary.

dips uniformly NE, and the trace of the foliation is slightly arched to broadly undulatory in cross-section (Fig. 5).

Minor structures within the zone consist of intrafolial folds, ptygmatic folds, and boudins (Fig. 6). Intrafolial folds occur in both the non-mylonitic and the mylonitic gneiss, but are much more common in the latter. No refolded folds were observed.

Various mylonitic microstructures occur throughout the zone, including retort-shaped, fractured and rotated porphyroclasts (Fig. 7a), and well-developed S- (*schistosité*) and C- (*cisaillement*) surfaces (Fig. 7b). Macroscopically visible C-surfaces occur only near the base of the shear zone. Here the foliation measured in the field corresponds to an S-surface, and the spaced C-surfaces produce slight normal offset of the S-surfaces. Structurally higher in the zone, S- and C-surfaces can be differentiated only microscopically. At this structural level, the macroscopic foliation does not correspond directly to an S- or a C-surface, but rather approximates the acute bisector of the microscopic surfaces. Throughout the zone, however, the C-surfaces dip more steeply northeast than the S-surfaces, consistently indicating a normal sense of shear. Quartz ribbons with oblique subgrains are ubiquitous, and consistently indicate a normal sense of shear (Fig. 7c).

Chemical analyses show that the deformation is isovolumetric, although some accessory minerals appear to have been unstable.

Two lozenges of non-mylonitic rock are enclosed within the mylonites, with mylonites both structurally above and below. In one case, the lozenge is completely surrounded by mylonitic gneiss (Figs. 3 and 5, section CC'). In the second case, the lozenge is continuous with the non-mylonitic rocks to the southwest, beyond the projected shear-zone boundary (Figs. 3 and 5, section

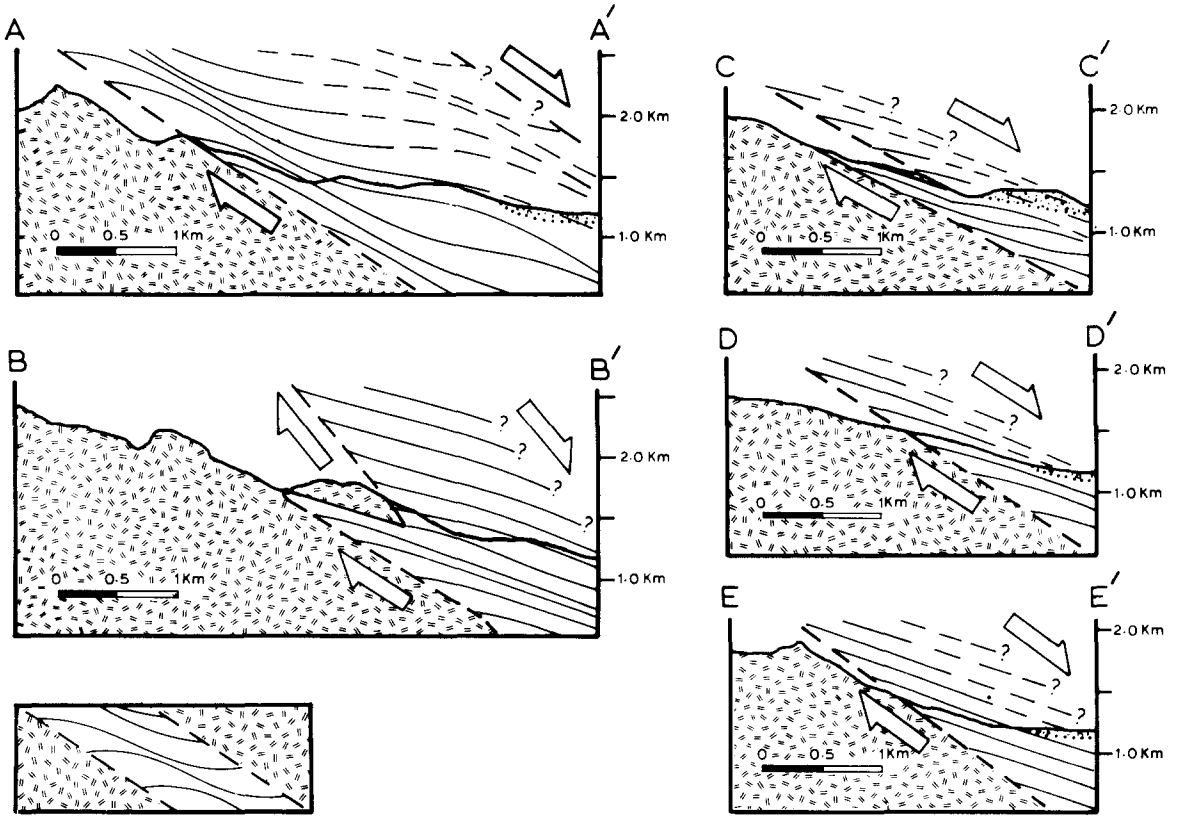

Fig. 5. Cross-sections parallel to mylonitic lineation. Solid lines represent observed and projected foliation traces. Light dashed lines represent the inferred upper part of the shear zone. Heavy dashed lines represent shear zone boundaries. Patterned area represents undifferentiated non-mylonitic rocks. Dotted pattern represents gravels. Inset in lower left depicts foliation geometry of idealized normal-displacement simple-shear zone.

BB'). The mylonites here are thus divisible into two sub-zones; an upper one which projects over the non-mylonitic rocks, and a lower one which tapers and pinches-out.

The upper boundary of the shear zone is not preserved. Typically the mylonites are depositionally overlain by unconsolidated gravels. Locally, they are structurally overlain by propylitically altered cataclasites derived from the mylonites.

Description of the mylonite zone boundary

The lower boundary to the mylonites is a 10–20 m thick zone characterized by numerous minor shear zones, faults, folds, and the absence of pervasive mylonitic foliation. The minor faults and shear zones occur primarily in the granite, granodiorite and quartzites. They are spaced at meter-scale intervals, strike NW sub-parallel to the mylonitic foliation, and dip NE slightly steeper than the foliation (Fig. 4d). The lineations within these minor zones have a trend of 040°, parallel to the main mylonitic lineation. Where the sense of displacement can be determined, either through offset markers or shear zone foliations, it is invariably normal (Fig. 8).

In the gneisses and schists of the boundary zone, the preexisting crystalloblastic foliation is crenulated, kinked, and isoclinally folded. Centimeter-scale kink folds are developed in the pelitic schist, and centimeter- to meter-scale, gently inclined and gently plunging class 2 or 3 isoclines (Ramsay 1967) are developed in the biotite schist (Fig. 9). The isoclines fold the crystalloblastic fabric, but lack a pervasive mylonitic fabric. The axial surfaces of both the kinks and the isoclines parallel the mylonitic foliation (Fig. 4d).

The fold axes cluster between 040 and 090° along a 300°, 20°NE great circle. The very similar orientations of the fold axes and the mylonitic lineation is not attributable to rotation by high shear strains. The absence of pervasive mylonitic foliation in the folded rocks indicates that the high strains required to produce such rotations ($\sim\gamma = 20$, Skjernaa, 1980) have not been attained. Rather, the axial orientations appear to correspond to the intersection of the surface being folded (i.e. the pre-shear crystalloblastic fabric) with the *ab* kinematic plane defined by the fold axial planes, consistent with interpretations of such folds as 'slip' or 'shear' folds (Ramsay 1967), or 'passive flow' folds (Donath and Parker 1964).

The attitude of the shear zone lower boundary, calculated from three-point geometric analyses, is remarkably uniform over the entire length of the zone (Fig. 4e). The lower boundary everywhere strikes sub-parallel to the mylonitic foliation, and dips NE slightly more steeply than the foliation (Fig. 5). Slight variations in attitude do occur, but these variations are systematic ones which define kilometer scale domains (Table 1). The narrow range of calculated attitudes within each domain indicates that the boundary within each is essentially planar.

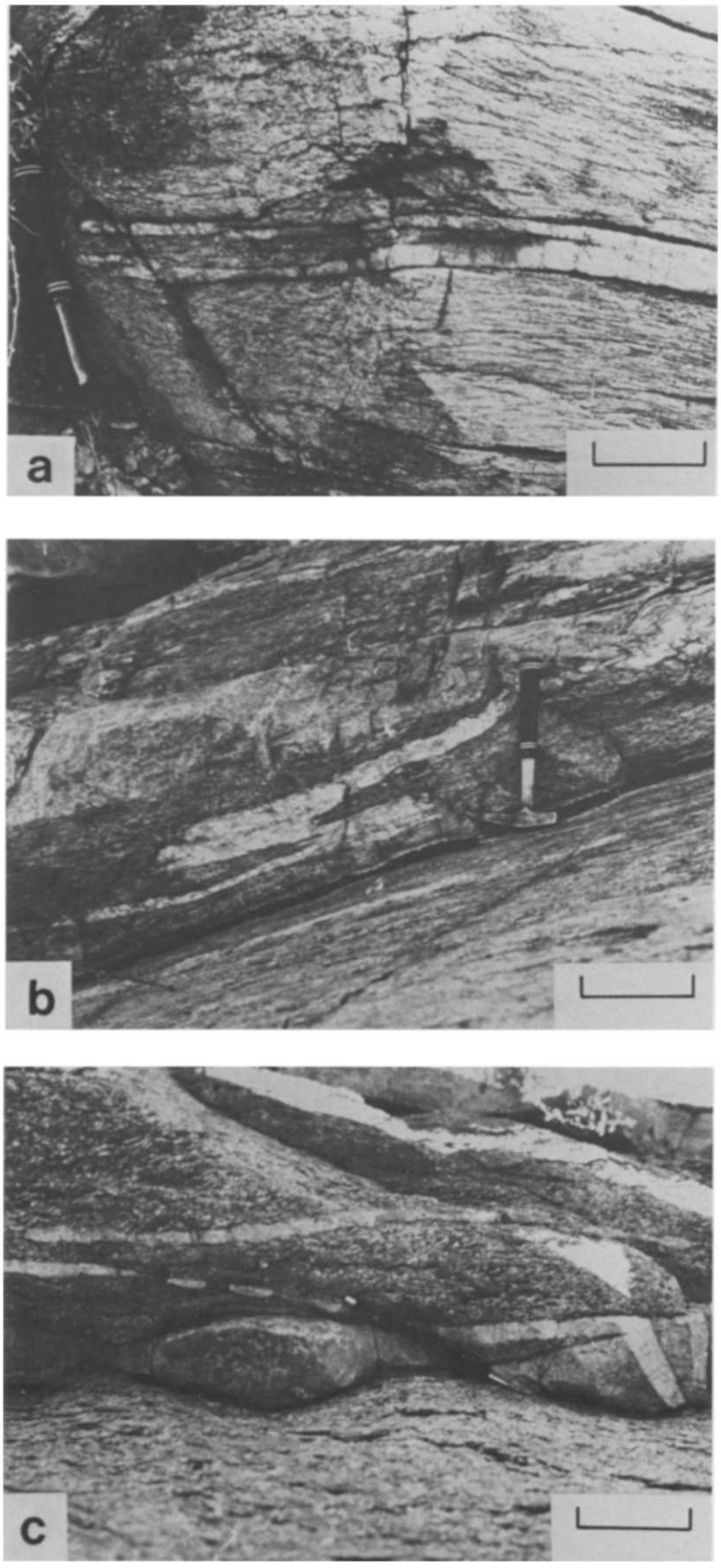

Fig. 6. Typical minor structures within the mylonites. (a) Intrafolially folded quartzite lamina. (b) Ptygmatically folded aplite dike with axial planar mylonitic foliation. (c) Boudins in a dike which has been rotated parallel to the mylonitic foliation. Scale bars are: (a) 7 cm; (b) 18 cm and (c) 7 cm.

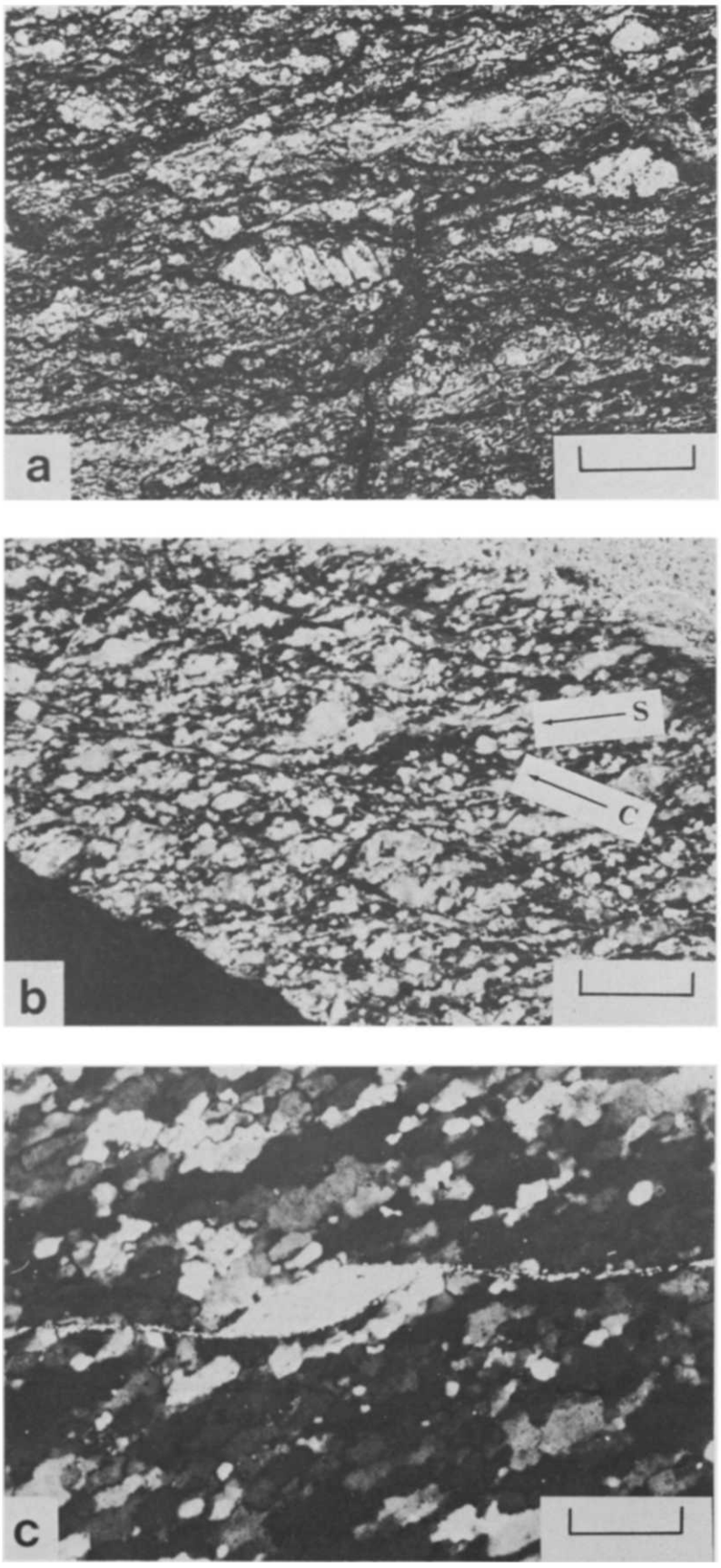

Fig. 7. Microstructures within the mylonites. (a) Retort-shaped, and fractured and rotated porphyroclasts in mylonitic orthogneiss. (b) S and C surfaces in mylonitic granite. (c) A muscovite porphyroclast and inclined quartz subgrains in a quartz ribbon. Scale bars are: (a) 2 cm; (b) 1 cm and (c) 170 μm.

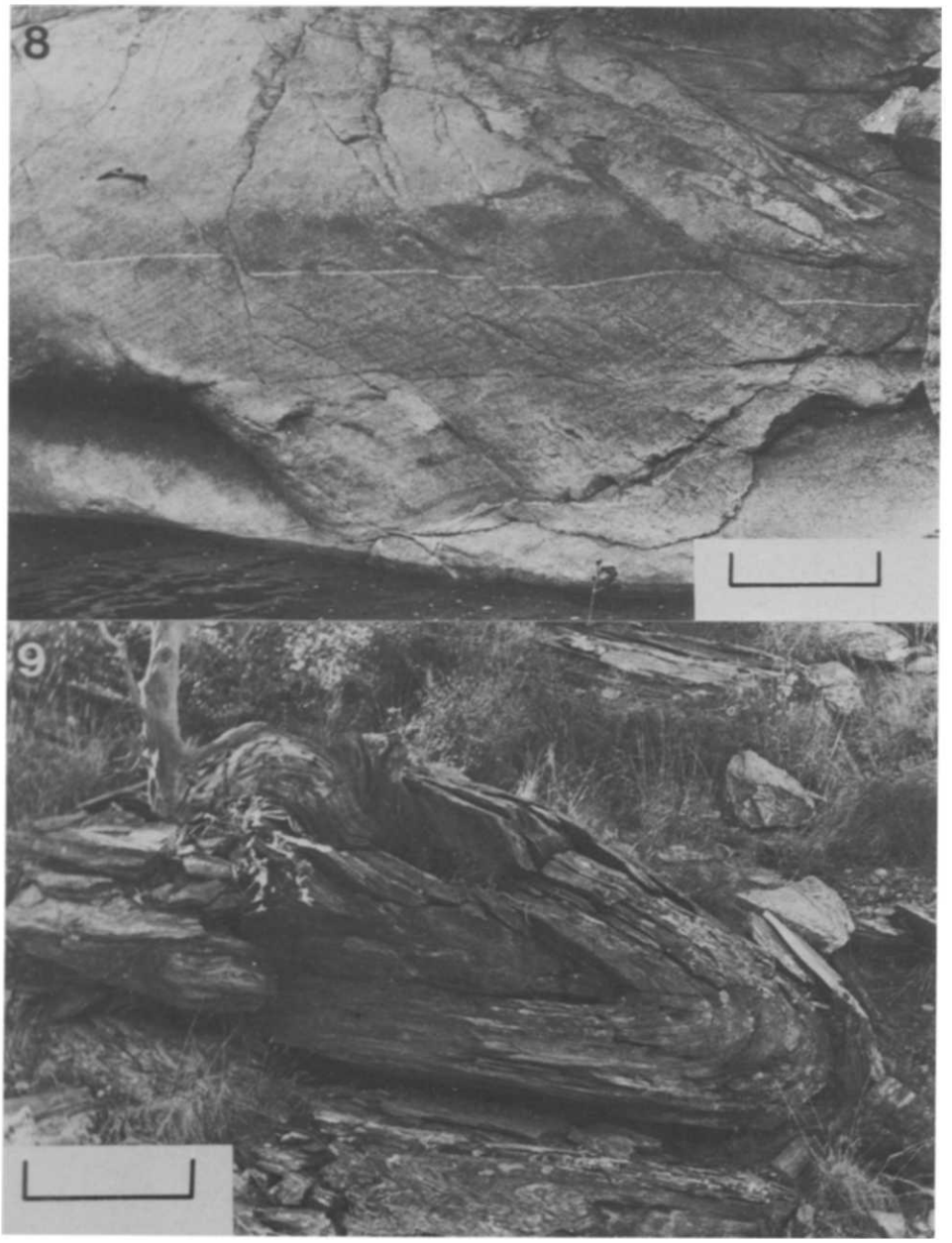

Fig. 8. Spaced shear-zones and faults offsetting an aplite dike in otherwise undeformed granite. Scale bar is 80 cm.

Fig. 9. Isocline in non-mylonitic biotite schist at the base of the shear zone. Scale bar is 40 cm.

Table 1. Summary of shear zone geometry

Domain	Cross-section	Mean lower boundary attitude	Mean θ'
I	AA′	299 ± 3°, 36 ± 3° NE	21 ± 9°
II	BB′	307°, 53° NE	31 ± 5°
III	CC′	292 ± 2°, 23 ± 1° NE	7 ± 4°
IV	DD′	292 ± 3°, 30 ± 4° NE	14 ± 5°
V	EE′	281 ± 9°, 33 ± 5° NE	19 ± 6°

KINEMATIC ANALYSIS OF THE MYLONITE ZONE

Evidence for normal-displacement simple shear

Abundant qualitative evidence indicates that the mylonites represent a normal-displacement ductile simple-shear zone. Vertical cross-sections parallel to the lineation show that the geometry of the zone is similar to that predicted for normal-displacement simple-shear zones. Even in the two domains where non-mylonitic rocks divide the mylonites into upper and lower zones, both zones have a normal sense of displacement.

The angular discordance between the foliation and the shear zone boundary precludes the possibility of the foliation being a slip plane, as discussed by Ramsay & Graham (1970). The occurrence of intrafolial folds within the mylonites, the occurrence of ptygmatic structures with axial planar mylonitic foliation, and the parallelism of fold axial surfaces and mylonitic foliation all strongly suggest that the mylonitic foliation represents the principal flattening plane. The boudinage of dikes which are parallel to the foliation is consistent with extension parallel to the mylonitic lineation, although it does not eliminate the possibility of extension in other directions as well.

The consistently steeper dip of 'slip-plane' indicators (fault planes, ultramylonite zones and shear zone boundaries) compared to 'strain-plane' indicators (fold axial surfaces and mylonitic foliation) suggests a normal sense of shear. Microstructures within the zone, including porphyroclasts, oblique subgrains, and S- and C-surfaces, all consistently indicate normal-displacement, non-coaxial shear (Simpson & Schmid 1983, Lister & Snoke 1984).

Strain calculations for domains of simple shear

While the entire Pinaleño Mountains mylonite zone generally appears to be a zone of normal-displacement simple-shear, three of the domains can be shown to be ones of plane-strain, simple shear in the most rigorous sense. In domains IV and V, values of shear strain calculated from the foliation geometry equal values calculated from the angular rotations of sheared lithologic contacts. The geometric similarity of domain I to domains IV and V indicate that it, too, is a domain of plane-strain simple shear.

In domain IV, a metasedimentary contact can be traced continuously from non-mylonitic rocks, across the boundary zone and into the shear zone. The initial orientation of the contact parallels the crystalloblastic foliation (025°, 18°SE). The final orientation of the contact (326°, 18°NE) can be calculated from its mapped trace (17°, 037°) and the intersection of the original contact with the shear zone boundary (295°, 31°NE). Assuming that the mylonitic foliation (303°, 18°NE) represents the XY plane of finite strain, with X parallel to the mylonitic lineation (18°, 040°), the principal strain ratios of the mylonitic deformation can be calculated from the above data and the following equations (Ramsay 1967, equations 4.21a–4.21c):

$$\left[\frac{\lambda_3}{\lambda_1}\right]^{1/2} = \frac{\tan \alpha_1'}{\tan \alpha_1}; \quad \left[\frac{\lambda_2}{\lambda_1}\right]^{1/2} = \frac{\tan \alpha_2'}{\tan \alpha_2}; \quad \left[\frac{\lambda_3}{\lambda_2}\right]^{1/2} = \frac{\tan \alpha_3'}{\tan \alpha_3}$$

where α_1 and α_1' equal the original and final angles between the X axis and the contact in the XZ principal plane; α_2 and α_2' equal the angles between X and the contact in the XY plane; and α_3 and α_3' equal the angles between Y and the contact in the YZ plane. The minimum and maximum X/Z ratios thus calculated from the rotated contact are 15/1 and 26/1, corresponding to shear strains of 3.6–4.9.

In the same domain, the angle (θ') between the mylonitic foliation and the shear-zone boundary ranges between 4 and 23° and has a mean value of 14 ± 5°. The values of shear strain (γ) calculated from the observed θ' values using equation (1) range between 1.9 and 14.2 and have a mean of 4.4 ± 2.8.

In domain V, as in the preceding domain, the mean strain calculated from the foliation attitudes (γ = 2.9; X/Z = 10/1) is in close agreement with the strain calculated from the rotation of a marker horizon (X/Z = 9/1). Thus in two separate domains, the shear strains calculated from θ' and equation (1) can be confirmed by independent calculations.

The geometry of domain I is very similar to that of domains IV and V (Table 1). The near-parallelism of boundary attitudes indicates that the shear couples are essentially parallel in each domain. The similarity of shear plane orientations and of θ' values suggests that θ' can be described by the same function in all three domains. Thus in domain I, as in the other two domains, θ' also appears to be exclusively a function of simple shear, and the shear strain consequently can be calculated from equation (1).

Shear strain distribution and translation estimates

To consider the shear strain distribution, rather than simply averages, γ can be calculated from the foliation attitudes for specific structural levels within each domain. Figures 10(a)–(c) are graphs of shear strain, as determined from foliation attitudes, vs height above the shear zone boundary as determined from cross-sections. The shear strain increases abruptly within a relatively small distance of the boundary, and is clearly heterogeneous. With regard to the heterogeneity, it is noteworthy that strains calculated from different points at the same height above the shear zone boundary, are in

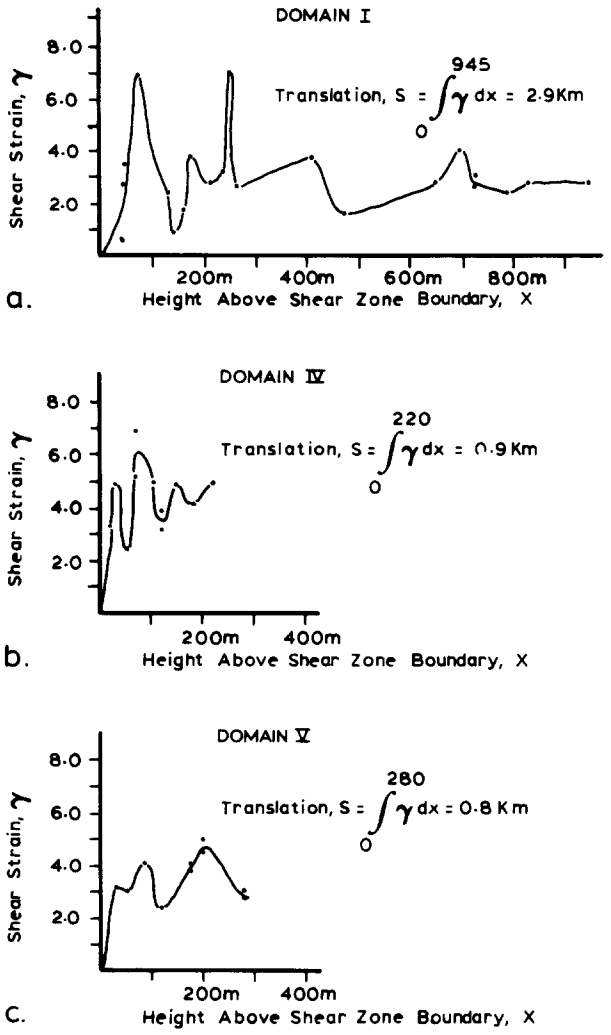

Fig. 10. Graphs of shear strain (γ) vs height above the shear zone lower boundary (x) for (a) domain I, (b) domain IV and (c) domain V. Translations are calculated from equation (2).

close agreement. In domain V, for example, two points with $x = 183$ m have shear strains of 3.8 and 4.1. Similar examples occur throughout the zone. It is also noteworthy that in the contiguous domains IV and V, the first four inflection points in the curves occur at the same value of x. This suggests that the variations in shear strain may be relatively large-scale features of the zone.

Translation estimates obtained by integrating the area under the curves in Fig. 10 range from 0.8 to 2.9 km. Because the upper boundary of the shear zone is not preserved, the zone's original width is unknown, and the calculated translations represent only minimum estimates. The variation among estimates is due primarily to differences in the preserved width of the zone, rather than to differences in shear strain.

The total displacement effected by the spaced faults and shears below the zone is an order of magnitude less than that effected by the shear zone itself. In the boundary zone of domain I, 24 normal faults and shear zones were measured in a 22 m long traverse. The average spacing of the faults was found to be 0.6 m, and the average displacement along them was found to be 0.3 m. Estimating the maximum extent of the faults to be on the order of 200 m, the total displacement effected by the faults can be approximated as

$$200 \text{ m} \times \frac{1 \text{ fault}}{0.6 \text{ m}} \times \frac{0.3 \text{ m displacement}}{\text{fault}}$$

$$= 100 \text{ m displacement.}$$

Strain relations at zone terminations

Domain II actually consists of two shear zones: a lower, 30°-dipping zone which tapers and terminates in the up-dip direction, and an upper, 50°-dipping zone whose termination is not apparent (Fig. 11). The foliation geometries in this domain resemble those predicted for shear zone terminations in general, and the merger of the two zones accords particularly well with the model described by Ramsay & Allison (1979) and Ramsay (1980) for the propagation of plane-strain shear zones (Fig. 12).

The crystalloblastic foliation below the termination of the lower shear zone in domain II strikes WNW and dips steeply S (Fig. 11). This is an anomalous orientation compared to the crystalloblastic foliation elsewhere within the range (see Fig. 4a). It does, however, coincide with the predicted orientation of flattening planes at that location within a shear zone termination. The ridge above the lower shear zone contains both a typical NE-striking, SE-dipping crystalloblastic foliation and widely spaced zones of NW-striking, NE-dipping

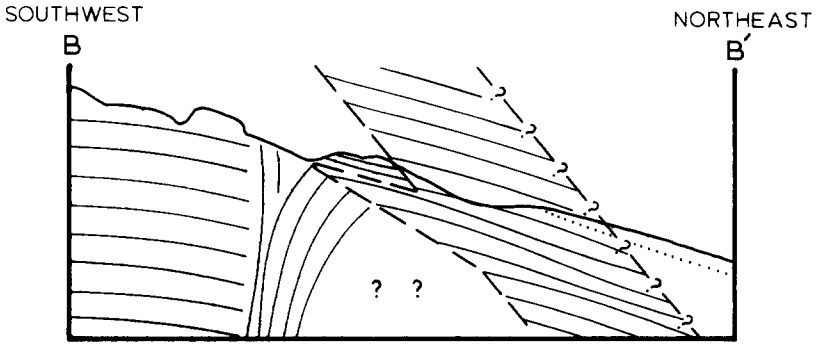

Fig. 11. Cross-section of domain II, showing observed foliation trajectories. Patterned areas denote areas of crystalloblastic or widely spaced mylonitic foliations (see text). Unpatterned areas denote areas of pervasive mylonitic foliation. The crystalloblastic foliation at the southwest end of the cross-section dips steeply southeast, but strikes subparallel to the section and hence appears horizontal in the plane of the section. Elsewhere the foliation strikes approximately perpendicular to the section.

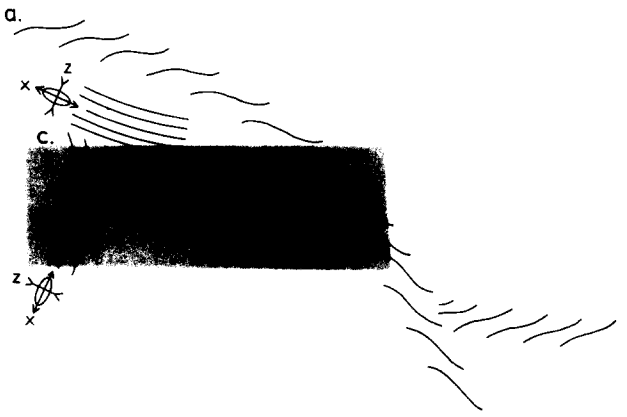

Fig. 12. Theoretical *XY* strain trajectories of two intersecting, right-handed, plane-strain shear zones (after Ramsay & Allison 1979, Ramsay 1980). Zone (a) offsets the lower zone at (b), which in turn is shown terminating at (c). The theoretical trajectories in the shaded area appear to correspond to the observed trajectories in Fig. 11.

mylonitic foliation. This latter foliation coincides with the predicted orientation of flattening planes at that relative location within a shear zone termination. Overall, this foliation geometry is consistent with the termination of either a plane-strain or a non-plane-strain shear zone. However, if the coalescing of similar-sense shear zones is a peculiarity of plane-strain zones, as suggested by Ramsay (1980), then the merger of the two zones suggests that they are zones of plane-strain deformation, consistent with the quantitative analysis described above.

SUMMARY

The major, minor, and microscopic scale structures of the Pinaleño Mountains mylonite zone uniformly indicate that the zone represents one of normal-displacement simple shear. Even where the zone bifurcates into an upper zone and a lower, terminated zone, the foliation geometries and the relative orientation of the zones correspond to the plane-strain shear-zone propagation model of Ramsay & Allison (1979).

The shear strains calculated assuming a simple-shear model equal the shear strains calculated from independent strain markers. The assumption that the deformation represents plane-strain simple shear thus appears well justified. In particular, the assumption that the macroscopic mylonitic foliation represents the *XY* plane of finite strain appears valid, despite the occurrence of S-C mylonites throughout the zone.

The actual values of shear strain ($\gamma = 3.5$) are surprisingly low, and thus appear to undermine the assumption that mylonites necessarily represent 'high' shear strains. The calculated displacement is similarly low (S = 2.9 km), but must be considered a minimum estimate because the total width of the zone is unknown.

Acknowledgements—Research funding was provided by an Arizona Bureau of Geology and Mineral Technology fellowship to the author, and National Science Foundation Grants EAR-8341222 and EAR-8206040 awarded to Dr. Roy Kligfield and Dr. George H. Davis.

REFERENCES

Bergquist, J. R. 1979. Reconnaissance geologic map of the Blue Jay Peak Quadrangle, Graham Co., Arizona. *U.S. geol. Surv. Misc. Field Studies Map* MF-1083.

Berthé, D., Choukroune, P. & Jegouzo, P. 1979. Orthogneiss, mylonite and non-coaxial deformational granites: the example of the South Armorican Shear Zone. *J. Struct. Geol.* **1**, 31–42.

Blacet, P. M. & Miller, S. T. 1978. Reconnaissance geologic map of the Jackson Mountain Quadrangle, Graham Co., Arizona. *U.S. geol. Surv. Misc. Field Studies Map* MF-939.

Brown, R. L. & Read, P. B. 1983. Shuswap terrane of British Columbia: a Mesozoic core complex. *Geology* **11**, 164–168.

Coney, P. J. 1980. Cordilleran metamorphic core complexes: an overview. In: *Cordilleran Metamorphic Core Complexes* (edited by Crittenden, M. D., Jr., Coney, P. J. & Davis, G. H.). *Mem. geol. Soc. Am.* **153**, 7–31.

Coward, M. P. 1976. Strain within ductile shear zones. *Tectonophysics* **34**, 181–197.

Davis, G. A., Anderson, J. L., Frost, E. G. & Shackelford, T. J. 1980. Mylonitization and detachment faulting in the Whipple-Buckskin-Rawhide Mountains terrane, southeastern California and western Arizona. In: *Cordilleran Metamorphic Core Complexes* (edited by Crittenden, M. D., Jr., Coney, P. J. & Davis, G. H.). *Mem. geol. Soc. Am.* **153**, 79–129.

Davis, G. H. 1980a. Structural characteristics of metamorphic core complexes, southern Arizona. In: *Cordilleran Metamorphic Core Complexes* (edited by Crittenden, M. D., Jr., Coney, P. J. & Davis, G. H.). *Mem. geol. Soc. Am.* **153**, 35–78.

Davis, G. H. 1980b. Metamorphic core complexes—structural characteristics, kinematic expression and relation to mid-Miocene listric faulting. In: *Cordilleran Metamorphic Core Complexes and Their Uranium Favorability* (edited by Coney, P. J. & Reynolds, S. J.). U.S. Dept. of Energy open file report GJBX-258(80).

Davis, G. H. 1983. Shear-zone model for the origin of metamorphic core complexes. *Geology* **11**, 342–347.

Davis, G. H. & Coney, P. J. 1979. Geological development of the Cordilleran metamorphic core complexes. *Geology* **7**, 120–124.

Davis, G. H. & Hardy, J. J., Jr. 1981. The Eagle Pass detachment, southeastern Arizona: product of mid-Miocene listric(?) normal faulting in the southern Basin and Range. *Bull. geol. Soc. Am.* **92**, 749–762.

Donath, F. A. & Parker, R. B. 1964. Folds and folding. *Bull. geol. Soc. Am.* **75**, 45–62.

Escher, A., Escher, J. C. & Watterson, J. 1975. The reorientation of the Kangamuit dike swarm, west Greenland. *Can. J. Earth Sci.* **12**, 158–173.

Kligfield, R., Carmignani, L. & Owens, W. H. 1981. Strain analysis of a Northern Apennine shear zone using deformed marble breccias. *J. Struct. Geol.* **3**, 421–435.

Lister, G. S. & Snoke, A. W. 1984. S-C mylonites. *J. Struct. Geol.* **6**, 617–638.

Miller, E. L., Gans, P. B. & Garing, J. 1983. The Snake River decollement: an exhumed Mid-Tertiary ductile–brittle transition. *Tectonics* **2**, 238–263.

Misch, P. 1960. Regional structural reconnaissance in central-northeast Nevada and some adjacent areas: observations and interpretations. *Intermountain Ass. Petrol. Geol. Guidebook for 11th Annual Field Conference*, 17–42.

Mitra, G. 1979. Ductile deformation zones in Blue Ridge basement rocks and estimation of finite strains. *Bull. geol. Soc. Am.* **90**, 935–951.

Ramsay, J. G. 1967. *Folding and Fracturing of Rocks*. McGraw-Hill, New York.

Ramsay, J. G. 1980. Shear zone geometry: a review. *J. Struct. Geol.* **2**, 83–99.

Ramsay, J. G. & Allison, I. 1979. Structural analysis of shear zones in an Alpinised Hercynian Granite. *Schweiz. miner. petrog. Mitt.* **59**, 251–279.

Ramsay, J. G. & Graham, R. H. 1970. Strain variation in shear belts. *Can. J. Earth Sci.* **7**, 786–813.

Rehrig, W. G. & Reynolds, S. J. 1980. Geological and geochronologic reconnaissance of a northwest-trending zone of metamorphic core complexes in southern and western Arizona. In: *Cordilleran Metamorphic Core Complexes* (edited by Crittenden, M. D., Jr., Coney, P. J. & Davis, G. H.). *Mem. geol. Soc. Am.* **153**, 131–158.

Simpson, C. & Schmid, S. M. 1983. An evaluation of criteria to deduce the sense of movement in sheared rocks. *Bull. geol. Soc. Am.* **94**, 1281–1288.

Skjernaa, L. 1980. Rotation and deformation of randomly oriented planar and linear structures in progressive simple shear. *J. Struct. Geol.* **2**, 101–109.

Spencer, J. E. 1984. Role of tectonic denudation in warping and uplift of low-angle normal faults. *Geology* **12**, 95–98.

Swan, M. M. 1976. The Stockton Pass Fault: an element of the Texas Lineament. Unpublished M.S. thesis, University of Arizona, Tucson, Arizona.

Thorman, C. H. 1982. Geology of the Pinaleño Mountains, Arizona: a preliminary report. *Arizona Geol. Soc. Digest* **13**, 5–12.